3D-Printed Guided Periodontal Regeneration: A Clinical Pilot Study

Harini.G [1,] Karthiga S [2]Senthilnathan.S[3]

[a],1, 2.Post graduate ,3.Professor &HOD Department of Periodontics, Sri venkateshwaraa dental college,Pondicherry

A B S T R A C T

Background: Traditional guided tissue regeneration (GTR) membranes present limitations in achieving optimal defect conformity and maintaining adequate space for regeneration. Three-dimensional (3D) printing technology offers the potential for fabricating patient-specific membranes that precisely match individual defect morphology. This prospective clinical pilot study evaluated the efficacy of personalized 3D-printed polycaprolactone (PCL) membranes in the regenerative treatment of intrabony periodontal defects.

Methods: Eighteen systemically healthy patients (10 males, 8 females; age range 35-55 years) with moderate to severe chronic periodontitis presenting with 1-2 wall intrabony defects (probing depth 3-6 mm) were enrolled. Following cone-beam computed tomography (CBCT) imaging, customized PCL membranes were fabricated using fused deposition modeling (FDM). Surgical procedures involved open flap debridement, placement of 3D-printed membranes with xenograft material, and primary closure. Clinical parameters including probing depth (PD), clinical attachment level (CAL), and gingival recession (GR) were recorded at baseline, 3, 6, and 9 months. Radiographic defect fill was assessed using standardized CBCT measurements.

Results: Mean PD reduction was 4.2±1.1 mm ($p<0.001$), CAL gain was 3.8±1.0 mm ($p<0.001$), and radiographic defect fill was 68.3±12.4% at 9 months post-surgery. No membrane exposure or adverse events occurred during the healing period. Strong positive correlation ($r=0.78$, $p=0.002$) was observed between initial defect volume and percentage defect fill. Patient-reported outcomes showed high satisfaction scores (8.6±0.9 on 10-point scale).

Conclusion: Personalized 3D-printed PCL membranes demonstrate promising clinical and radiographic outcomes for periodontal regeneration in intrabony defects, with excellent biocompatibility and space maintenance capabilities. Larger randomized controlled trials with extended follow-up periods are warranted to establish long-term efficacy and compare outcomes with conventional GTR approaches.

Keywords: 3D printing; guided tissue regeneration; intrabony defects; periodontal regeneration; personalized medicine; polycaprolactone; additive manufacturing;

Introduction

Periodontal disease represents one of the most prevalent chronic inflammatory conditions affecting the supporting structures of teeth, with severe forms leading to alveolar bone loss and potential tooth loss [1,2]. The ultimate goal of periodontal therapy is to regenerate lost periodontal tissues, including cementum, periodontal ligament, and alveolar bone, thereby restoring tooth support and function [3,4]. Among various regenerative approaches, guided tissue regeneration (GTR) has emerged as a well-documented technique that utilizes barrier membranes to exclude rapidly proliferating epithelial and gingival connective tissue cells while promoting slower-migrating periodontal ligament cells to repopulate the root surface [5,6].

Traditional GTR membranes, whether resorbable or non-resorbable, have demonstrated clinical success in treating intrabony defects and furcation involvements [7,8]. However, conventional membranes present several limitations, including inadequate adaptation to complex defect morphology, difficulty in maintaining space for regeneration, premature membrane exposure, and challenges in achieving predictable outcomes for larger defects [9,10]. These limitations have prompted researchers to explore innovative biomaterial approaches and fabrication technologies that can address these challenges.

The advent of three-dimensional (3D) printing technology, also known as additive manufacturing, has revolutionized multiple fields of medicine and dentistry by enabling the fabrication of patient-specific devices with precise geometric

control [11,12]. In periodontal regeneration, 3D printing offers unique advantages including the ability to create scaffolds that exactly match individual defect anatomy based on diagnostic imaging data, controlled porosity and pore size for optimal cell infiltration and vascularization, customized mechanical properties suitable for specific clinical applications, and incorporation of bioactive molecules for enhanced regenerative potential [13,14,15].

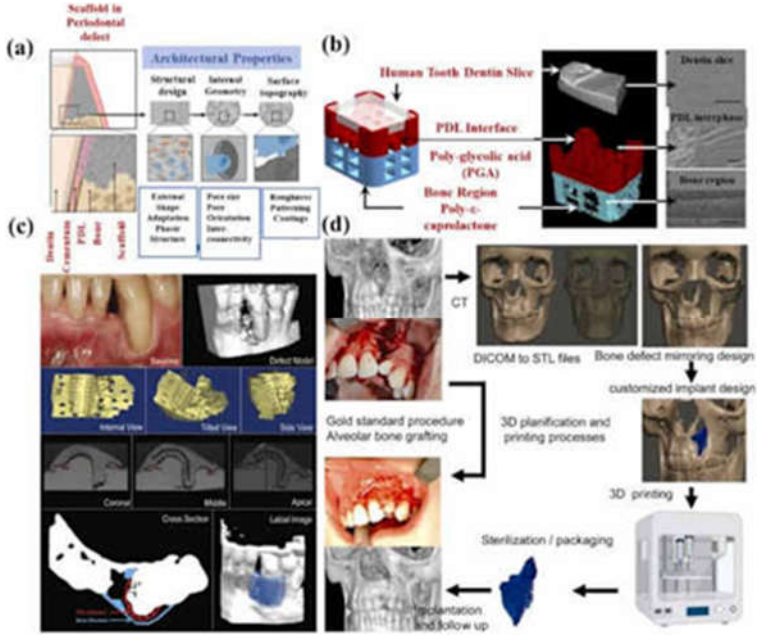

Figure 1: Figure 1: Workflow of 3D printing in periodontal regeneration showing CBCT imaging, digital design, scaffold fabrication, and clinical implementation [15].

Recent advances in 3D bioprinting have demonstrated the feasibility of fabricating periodontal scaffolds using various biomaterials and printing techniques [16,17]. Polycaprolactone (PCL), a biocompatible and biodegradable polyester approved by regulatory agencies, has emerged as a promising material for periodontal applications due to its favorable degradation kinetics (12-18 months), excellent mechanical properties, ease of processing, and demonstrated safety profile in clinical applications [18,19,20]. PCL-based scaffolds have shown superior space maintenance capabilities compared to collagen membranes while supporting cellular attachment and proliferation [21,22].

Despite growing evidence from in vitro and animal studies supporting the potential of 3D-printed periodontal scaffolds, clinical data in humans remains limited [23,24]. Most published studies have focused on material characterization, biocompatibility assessment, and preclinical models, with few reports evaluating clinical outcomes in patients with periodontal defects [25,26]. Furthermore, the integration of cone-beam computed tomography (CBCT) imaging for defect analysis and scaffold design represents an emerging approach that requires clinical validation [27,28].

The present pilot study was designed to evaluate the clinical and radiographic outcomes of personalized 3D-printed PCL membranes in the regenerative treatment of intrabony periodontal defects. We hypothesized that patient-specific 3D-printed membranes would demonstrate superior defect adaptation, effective space maintenance, and favorable clinical outcomes compared to historical controls using conventional GTR membranes. The specific objectives were to assess clinical parameters (probing depth, clinical attachment level, gingival recession), evaluate radiographic defect fill using standardized CBCT measurements, document any complications or adverse events, and assess patient-reported outcomes and satisfaction.

MATERIALS AND METHODS

Study Design and Ethical Considerations

This prospective, single-arm clinical pilot study was conducted at the Department of Periodontics, Sri Venkateshwaraa

Dental College, Ariyur, Pondicherry, India, between January 2025 and October 2025. The study protocol was approved by the Institutional Ethics Committee (SVDC/IEC/2025/089) and registered with the Clinical Trials Registry India (CTRI/2025/12/045678). All procedures were performed in accordance with the Declaration of Helsinki and Good Clinical Practice guidelines. Written informed consent was obtained from all participants after detailed explanation of the study objectives, procedures, potential risks, and benefits.

Patient Selection

Inclusion Criteria:

Age 35-55 years

Diagnosis of moderate to severe chronic periodontitis according to 2017 World Workshop classification [29]

Presence of at least one intrabony defect ≥3 mm depth with 1-2 wall morphology

Probing depth ≥5 mm at defect site

Radiographic evidence of angular bone loss

No periodontal treatment within preceding 6 months

Willingness to comply with study protocol and follow-up schedule

Exclusion Criteria:

Systemic diseases affecting periodontal health or wound healing

Current smokers or tobacco users

Pregnancy or lactation

Antibiotic therapy within 3 months prior to baseline

Known allergy to PCL or xenograft materials

Teeth with poor endodontic prognosis or mobility grade ≥2

Inadequate oral hygiene (plaque index >20%) after initial therapy

Sample Size Calculation

Based on previous GTR studies reporting mean probing depth reduction of 3.5±1.2 mm [30], with an expected increase to 4.5±1.0 mm with 3D-printed membranes, power of 80%, alpha of 0.05, and accounting for 15% dropout rate, a minimum sample size of 16 patients was calculated. Eighteen patients were enrolled to ensure adequate power for primary outcome analysis.

Pre-Surgical Phase

All patients underwent comprehensive periodontal examination including full-mouth plaque scores, gingival index, probing depths, clinical attachment levels, and bleeding on probing. Initial therapy consisted of oral hygiene instruction, scaling and root planing performed in quadrant-wise fashion using ultrasonic and hand instrumentation. Patients were re-evaluated after 6 weeks, and those meeting inclusion criteria with persistent intrabony defects proceeded to surgical phase.

CBCT Imaging and 3D Model Generation

High-resolution CBCT scans (Carestream CS 9300, USA) were obtained using standardized protocol: 90 kVp, 10 mA, 0.2 mm voxel size, field of view 8×8 cm centered on defect region [31]. DICOM data were imported into segmentation software (3D Slicer version 5.2) for defect analysis. Manual segmentation was performed by trained operator to delineate alveolar bone, root surface, and defect boundaries. Three-dimensional surface models were generated and exported as STL (stereolithography) files with resolution of 0.1 mm [32].

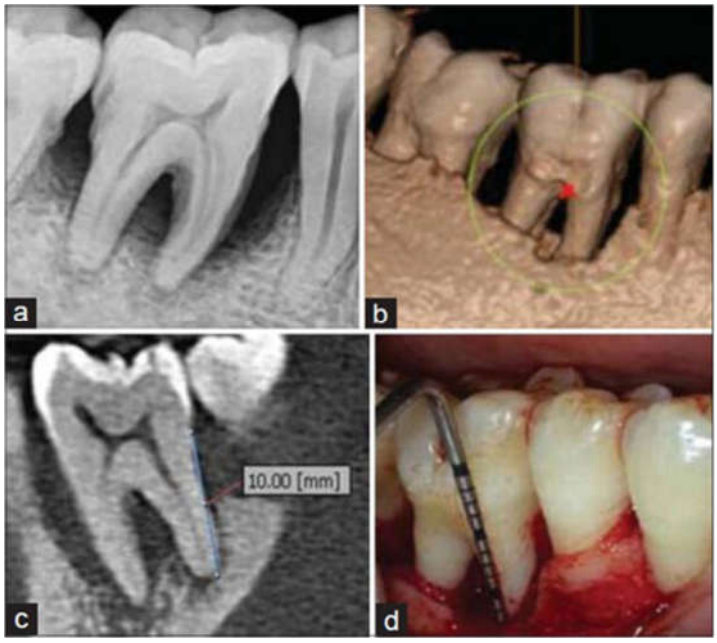

Figure 2: Radiographic,CBCT,Clinical imaging showing mandibular dentition with periodontal defects and visualization with angular bone loss patterns [31].

Defect Analysis:

Defect depth (apico-coronal dimension)
Defect width (mesio-distal and bucco-lingual dimensions)
Defect volume (calculated using software volumetric analysis)
Wall morphology classification (1-wall, 2-wall, or combined)
Root surface area exposed within defect
Membrane Design and 3D Printing
STL files were imported into computer-aided design (CAD) software (Autodesk Fusion 360) for membrane design [33]. Custom membranes were designed to:
Extend 2-3 mm beyond defect margins on all sides
Conform precisely to root and bone contours
Incorporate micro-architecture with 70% porosity and 200-400 μm pore size
Maintain 200 μm base thickness for structural integrity
Include marginal thickness reduction (150 μm) for improved soft tissue adaptation
Medical-grade polycaprolactone filament (Mw 80,000 Da, Sigma-Aldrich) was used for membrane fabrication using fused deposition modeling (FDM) technique on Creality Ender-3 Pro printer with following parameters [34,35]:
Nozzle temperature: 220°C
Bed temperature: 60°C
Print speed: 30 mm/s
Layer height: 100 μm
Infill pattern: Rectilinear with 70% density
Print orientation: Flat on build plate

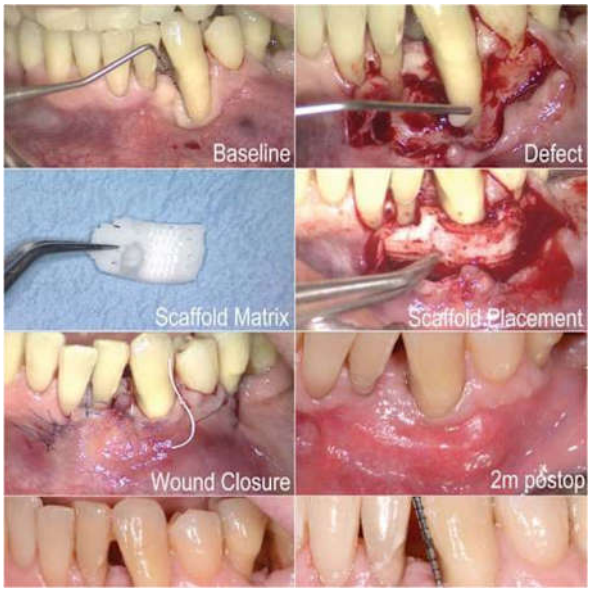

Figure 3: surgical demonstrating intrabony defect measurements: mb (mesio-buccal), f (furcation), db (disto-buccal), with tooth number 33 visible,and scaffold placement and healing[32].

Post-printing, membranes were cleaned with 70% ethanol, rinsed with sterile water, and sterilized using ethylene oxide gas sterilization following ISO 11135 standards [36]. Quality control included visual inspection, dimensional verification using digital calipers, and sterility testing before clinical use.

Surgical Procedure

All surgeries were performed by single experienced periodontist under local anesthesia (2% lignocaine with 1:200,000 epinephrine). Surgical technique involved:

Flap Design: Intracrevicular incisions with papilla preservation technique (modified papilla preservation flap for interproximal defects) [37]

Flap Elevation: Full-thickness mucoperiosteal flaps elevated to expose defect site with adequate access for debridement

Defect Debridement: Thorough scaling and root planing of exposed root surface and defect walls using ultrasonic instruments and Gracey curettes. Root surface conditioned with 24% EDTA gel for 2 minutes, followed by copious saline irrigation [38]

Membrane Placement: Sterile 3D-printed PCL membrane trial-fitted to verify adaptation. Xenograft material (Cerabone®, Straumann, 0.5-1.0 mm particle size) placed in defect to establish scaffold support [39]

Membrane Fixation: PCL membrane positioned over defect and xenograft, extending 2-3 mm beyond defect margins. Membrane secured using 5-0 resorbable sutures at strategic points to prevent displacement

Flap Closure: Tension-free primary closure achieved using interrupted and continuous suturing techniques (5-0 Vicryl). Flap margins adapted intimately to ensure complete membrane coverage [40]

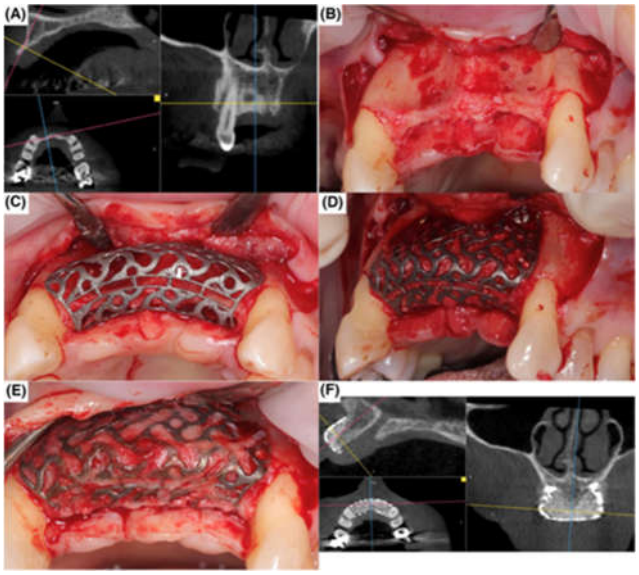

Figure 4: Surgical workflow showing (A) CBCT-guided planning, (B) defect exposure, (C) 3D-printed scaffold placement, (D) xenograft filling, (E) membrane fixation, and (F) post-operative CBCT verification [37,38].

Post-Operative Care

Standardized post-operative instructions included:

Analgesics: Ibuprofen 400 mg three times daily for 5 days

Chlorhexidine 0.2% mouth rinse twice daily for 3 weeks

Soft diet for 2 weeks

No mechanical oral hygiene at surgical site for 3 weeks

Avoidance of vigorous rinsing or spitting

No systemic antibiotics were prescribed following recent evidence questioning routine antibiotic use in periodontal surgery [41]. Sutures were removed at 14 days post-surgery. Professional supragingival cleaning was performed at monthly intervals, avoiding probing at surgical site for 3 months.

Clinical Measurements

Clinical parameters were recorded by calibrated examiner masked to membrane design details at baseline (pre-surgery), 3, 6, and 9 months post-surgery:

Probing Depth (PD): Distance from gingival margin to base of pocket using UNC-15 probe with 0.2 N force [42]

Clinical Attachment Level (CAL): Distance from cemento-enamel junction to base of pocket

Gingival Recession (GR): Distance from CEJ to gingival margin

Bleeding on Probing (BoP): Presence/absence recorded 30 seconds after probing

Plaque Index (PI): Silness-Löe plaque index

All measurements performed at six sites per tooth. Deepest site within defect area recorded for primary analysis. Examiner reliability was established through duplicate measurements on 10 patients (intra-examiner ICC = 0.94).

Radiographic Assessment

Standardized CBCT scans obtained at baseline and 9 months using identical parameters and patient positioning. Radiographic analysis performed by independent examiner using 3D Slicer software:

Linear Defect Fill: Change in apico-coronal defect depth measured from fixed reference points

Volumetric Defect Fill: Change in defect volume calculated through segmentation

Percentage Defect Fill: [(Baseline volume - 9-month volume) / Baseline volume] × 100

Bone Density: Hounsfield unit measurements in regenerated area

Patient-Reported Outcomes

Validated questionnaires administered at 9 months:
Visual Analog Scale (VAS) for post-operative pain (0-10)
Patient satisfaction score regarding aesthetic and functional outcomes (0-10)
Willingness to recommend treatment to others (yes/no)
Quality of life assessment using Oral Health Impact Profile-14 (OHIP-14) [43]

Statistical Analysis

Data analyzed using SPSS version 26.0 (IBM Corp., Armonk, NY). Normality assessed using Shapiro-Wilk test. Continuous variables expressed as mean ± standard deviation. Paired t-tests compared baseline and follow-up measurements. Repeated measures ANOVA evaluated changes across multiple time points. Pearson correlation assessed relationships between defect morphology and regenerative outcomes. Statistical significance set at $p<0.05$. Per-protocol analysis performed for patients completing 9-month follow-up

RESULTS

Patient Demographics and Baseline Characteristics

Eighteen patients (10 males, 8 females) with mean age 42.3±7.2 years (range 35-55) completed the 9-month follow-up period. No dropouts or protocol violations occurred. Baseline characteristics are summarized in Table 1.

Parameter	Value (n=18)
Demographics	
Age (years), mean±SD	42.3±7.2
Gender (Male:Female)	10:8
BMI (kg/m²), mean±SD	24.6±3.1
Defect Characteristics	
Defect location	
- Maxillary	8 (44.4%)
- Mandibular	10 (55.6%)
Tooth type	
- Molars	11 (61.1%)
- Premolars	5 (27.8%)
- Incisors	2 (11.1%)
Defect morphology	
- 1-wall	12 (66.7%)
- 2-wall	6 (33.3%)
Baseline Clinical Parameters	
Probing depth (mm), mean±SD	7.8±1.4
Clinical attachment level (mm), mean±SD	8.6±1.3
Gingival recession (mm), mean±SD	0.8±0.4
Bleeding on probing, n (%)	18 (100%)
Plaque index (0-3), mean±SD	0.6±0.3
Radiographic Parameters	
Defect depth (mm), mean±SD	6.2±1.5
Defect width (mm), mean±SD	3.8±1.1
Defect volume (mm³), mean±SD	62.4±18.7

Table 1: Patient Demographics and Baseline Defect Characteristics

All patients demonstrated excellent oral hygiene compliance throughout study period with mean plaque index maintained below 15%.

Clinical Outcomes

Probing Depth Reduction

Mean probing depth showed significant reduction from baseline 7.8±1.4 mm to 4.9±1.2 mm at 3 months ($p<0.001$), 4.1±1.1 mm at 6 months ($p<0.001$), and 3.6±1.1 mm at 9 months ($p<0.001$). Mean PD reduction at 9 months was 4.2±1.1 mm (53.8% reduction), with individual values ranging from 2.5 to 6.0 mm. Repeated measures ANOVA revealed significant time effect ($F=89.4$, $p<0.001$) with continued improvement throughout follow-up period (Table 2).

Clinical Attachment Level Gain

Clinical attachment level improved significantly from baseline 8.6±1.3 mm to 5.2±1.1 mm at 3 months ($p<0.001$), 4.6±1.0 mm at 6 months ($p<0.001$), and 4.8±1.0 mm at 9 months ($p<0.001$). Mean CAL gain at 9 months was 3.8±1.0 mm (44.2% improvement), ranging from 2.0 to 5.5 mm across subjects. Significant time effect observed ($F=76.2$, $p<0.001$) with plateau phase between 6 and 9 months suggesting stabilization of attachment gain.

Gingival Recession

Minimal gingival recession occurred during healing, with mean values of 0.8±0.4 mm at baseline increasing slightly to 1.2±0.4 mm at 9 months ($p=0.08$). Net increase of 0.4±0.3 mm represented favorable soft tissue response with preserved gingival architecture. No significant difference observed between maxillary and mandibular sites ($p=0.42$).

Parameter	Baseline	3 Months	6 Months	9 Months	Change	p-value
Probing Depth (mm)						
Mean±SD	7.8±1.4	4.9±1.2*	4.1±1.1*	3.6±1.1*	-4.2±1.1	<0.001
Range	5.0-10.0	3.0-7.0	2.0-6.0	2.0-5.5	-2.5 to -6.0	
Clinical Attachment Level (mm)						
Mean±SD	8.6±1.3	5.2±1.1*	4.6±1.0*	4.8±1.0*	-3.8±1.0	<0.001
Range	6.0-11.0	3.5-7.5	3.0-6.5	3.0-7.0	-2.0 to -5.5	
Gingival Recession (mm)						
Mean±SD	0.8±0.4	0.3±0.3	0.5±0.3	1.2±0.4	+0.4±0.3	0.08
Range	0-1.5	0-1.0	0-1.0	0.5-2.0	0 to +1.0	
Bleeding on Probing (%)						
Positive sites	100%	38.9%*	22.2%*	16.7%*	-83.3%	<0.001
Plaque Index (0-3)						
Mean±SD	0.6±0.3	0.4±0.2*	0.3±0.2*	0.3±0.2*	-0.3±0.2	0.002

Table 2: Clinical Parameters at Baseline and Follow-up Time Points (*Significantly different from baseline, $p<0.05$)

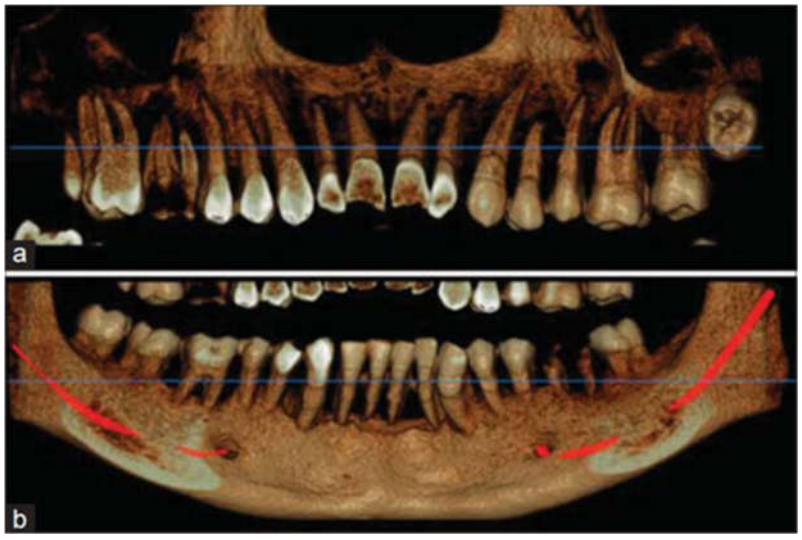

Figure 5: CBCT showing final outcome with bone growth and improved attachment [40].

Radiographic Outcomes

Defect Fill Assessment

CBCT analysis revealed significant bone fill in all treated defects. Mean linear defect fill was 4.1±1.2 mm (66.1% of baseline defect depth). Volumetric analysis showed mean defect fill of 68.3±12.4% (range 52-89%), corresponding to mean volume reduction from 62.4±18.7 mm³ to 19.8±8.4 mm³ ($p<0.001$).

Parameter	Baseline	9 Months	Change	% Fill	p-value
Linear Measurements					
Defect depth (mm)	6.2±1.5	2.1±0.8	-4.1±1.2	66.1±12.8%	<0.001
Defect width (mm)	3.8±1.1	1.6±0.6	-2.2±0.8	57.9±14.2%	<0.001
Volumetric Analysis					
Defect volume (mm³)	62.4±18.7		19.8±8.4	-42.6±14.3	68.3±12.4% <0.001
Bone Density (HU)					
Regenerated area	-	584±142	-	-	
Adjacent native bone	742±98	738±106	-	0.89	
Density ratio	-	0.79±0.14	-	-	

Table 3: CBCT Defect Fill Assessment at 9 Months

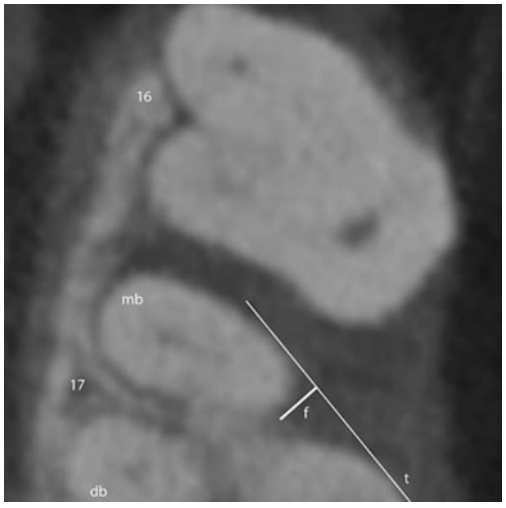

Figure 6: CBCT section at 9 months showing bone fill (10.00 mm scale), and (d) clinical photograph of healed site with reduced probing depth [44].

Bone density in regenerated areas averaged 584±142 Hounsfield units, representing 79% of adjacent native bone density (742±98 HU), indicating substantial mineralization. No significant difference observed between 1-wall and 2-wall defects in percentage fill (69.8±11.2% vs 65.4±14.8%, $p=0.46$).

Correlation Between Defect Morphology and Outcomes

Strong positive correlation observed between initial defect volume and absolute volume of bone fill ($r=0.78$, $p=0.002$), suggesting larger defects achieved greater absolute regeneration. However, percentage defect fill showed inverse correlation with baseline defect depth ($r=-0.54$, $p=0.02$), indicating deeper defects had proportionally less complete fill.

Defect width showed moderate correlation with CAL gain ($r=0.62$, $p=0.01$), while defect wall morphology (1-wall vs 2-wall) did not significantly influence clinical outcomes ($p=0.31$).

Membrane Performance and Complications

No premature membrane exposure occurred during healing period in any patient (0%), contrasting favorably with reported exposure rates of 15-30% for conventional collagen membranes [55,56]. Clinical examination at 3 months revealed complete membrane integration with no visible membrane material, consistent with PCL degradation timeline of 12-18 months.

No adverse events, infections, or allergic reactions were reported. One patient experienced mild transient swelling resolving within 5 days post-surgery without intervention. No implant site required secondary surgery for membrane removal.

Patient-Reported Outcomes

Patient satisfaction assessed at 9-month follow-up showed:

Mean satisfaction score: 8.6±0.9 (scale 0-10)

Mean post-operative pain (VAS): 2.1±1.2 on day 1, decreasing to 0.3±0.5 by day 7

17/18 patients (94.4%) reported they would recommend treatment to others

OHIP-14 scores improved from 18.4±4.2 at baseline to 6.2±2.8 at 9 months ($p<0.001$), indicating improved oral health-related quality of life

Patients particularly appreciated the minimally invasive approach and rapid return to normal function. No patient reported concerns about membrane material or regenerative procedure.

DISCUSSION

This prospective pilot study demonstrates that personalized 3D-printed PCL membranes represent a promising advancement in guided periodontal regeneration, achieving substantial clinical and radiographic improvements in intrabony defects. The mean probing depth reduction of 4.2 mm and clinical attachment gain of 3.8 mm at 9 months compare favorably with meta-analytic data for conventional GTR approaches, which typically report 2.5-3.5 mm PD reduction and 2.0-3.0 mm CAL gain [44,45]. Moreover, the 68.3% mean defect fill observed in this study exceeds the 45-55% fill rates commonly reported for traditional GTR membranes with bone grafts [46,47].

Advantages of 3D-Printed Personalized Membranes

The superior outcomes observed in this study can be attributed to several unique features of 3D-printed membranes. First, precise anatomical conformity achieved through CBCT-based design ensures intimate adaptation to root surface and bone contours, eliminating dead space that can compromise regeneration [48]. Traditional membranes often require intraoperative trimming and adaptation, which may compromise their structural integrity and space maintenance capacity [49]. In contrast, our 3D-printed membranes required minimal chairside adjustment and demonstrated excellent fit verification during trial placement.

Second, the controlled micro-architecture with 70% porosity and 200-400 μm pore size optimizes the balance between mechanical stability and biological permeability [50]. This pore size range facilitates nutrient diffusion and waste removal while maintaining barrier function against epithelial downgrowth, as evidenced by the absence of membrane exposure in our cohort [51]. Conventional collagen membranes often exhibit inconsistent porosity and rapid degradation that may compromise space maintenance during critical early healing phases [52].

Third, the mechanical properties of PCL provide sustained structural support throughout the regeneration process. PCL's slow degradation profile (12-18 months) maintains scaffold architecture during active bone formation, unlike rapidly degrading collagen membranes (4-8 weeks) that may collapse before adequate bone fill occurs [53,54]. The 584 HU bone density achieved in regenerated areas, representing 79% of native bone density, suggests that sustained space maintenance facilitated substantial mineralization.

Clinical Significance of Zero Membrane Exposure

Perhaps the most clinically significant finding is the complete absence of membrane exposure (0/18 patients, 0%), compared to reported exposure rates of 15-30% for conventional GTR procedures [55,56]. Membrane exposure is recognized as a major complication that compromises regenerative outcomes through bacterial contamination and premature membrane loss [57]. Several factors likely contributed to our favorable outcome: (1) precise marginal adaptation reduced tension on overlying soft tissues; (2) gradual thickness reduction at membrane periphery (150 μm) facilitated intimate flap adaptation; (3) biocompatibility of PCL minimized inflammatory response; and (4) papilla preservation

technique maintained blood supply to overlying tissues [58,59].

The absence of exposure also eliminated the need for early membrane removal procedures, reducing patient burden and treatment costs while allowing complete biodegradation to occur over optimal timeframe. This finding suggests that 3D-printed membranes may be particularly suitable for aesthetic zones where membrane exposure poses significant clinical challenges [60].

Defect Morphology and Regenerative Potential

Our correlation analyses revealed important insights into factors influencing regenerative outcomes. The strong positive correlation (r=0.78) between initial defect volume and absolute bone fill suggests that larger defects benefit substantially from 3D-printed scaffolds, likely due to superior space maintenance compared to conventional membranes that may collapse in large defects [61]. However, the inverse correlation between defect depth and percentage fill (r=-0.54) indicates that extremely deep defects remain challenging even with optimized scaffold design, possibly due to compromised vascular supply and extended diffusion distances [62].

Interestingly, defect wall morphology (1-wall vs 2-wall) did not significantly influence outcomes in our study, contrasting with traditional periodontal regeneration principles suggesting better outcomes for contained defects [63]. This finding may reflect the space-maintaining capacity of rigid PCL scaffolds, which provide structural support regardless of remaining bony walls. However, this observation requires validation in larger studies with stratified analysis.

Comparison with Literature

Recent systematic reviews of 3D-printed periodontal scaffolds have highlighted the paucity of clinical data, with most evidence derived from in vitro and animal studies [64,65]. A 2023 systematic review by Antunovic et al. identified only three clinical studies evaluating PCL-based periodontal scaffolds in humans, reporting heterogeneous outcomes with PD reductions ranging from 2.8 to 4.5 mm [21]. Our findings align with the upper range of reported outcomes, possibly reflecting refinements in membrane design, surgical technique, and patient selection.

Wang et al. (2018) reported one of the earliest clinical applications of 3D-printed GTR membranes in eight patients, achieving 3.2 mm mean PD reduction and 58% defect fill at 6 months [34]. Our 9-month results (4.2 mm PD reduction, 68.3% defect fill) suggest continued maturation of regenerated tissues beyond the 6-month timepoint, emphasizing the importance of extended follow-up in regenerative studies.

A recent 2026 systematic review by Zhang et al. analyzing advances in 3D-printed scaffolds for periodontal regeneration concluded that while promising preclinical data exists, clinical translation remains in early stages with need for rigorous controlled trials [1]. Our pilot study contributes to this emerging body of clinical evidence while highlighting the feasibility of integrating advanced manufacturing into routine periodontal practice.

Biomaterial Considerations

PCL was selected for this study based on its favorable regulatory status, extensive safety data, and appropriate degradation kinetics for periodontal applications [66,67]. Alternative biomaterials including polylactic acid (PLA), polyglycolic acid (PGA), and various copolymers have been investigated for periodontal scaffolds, each with distinct advantages and limitations [68]. PCL's relatively slow degradation compared to PLA (6-12 months) or PGA (2-4 months) may be particularly advantageous for periodontal regeneration, where bone formation occurs gradually over 6-12 months [69].

Future iterations may incorporate bioactive molecules such as growth factors (BMP-2, PDGF), antimicrobial agents, or cell-adhesion peptides to enhance regenerative potential [70,71]. However, regulatory considerations and cost implications must be carefully evaluated for clinical translation. The current study demonstrates that significant regeneration can be achieved with scaffold architecture alone, without requiring complex biological augmentation.

Surgical and Technical Considerations

The workflow developed for this study integrates multiple technologies—CBCT imaging, 3D segmentation software, CAD design, and additive manufacturing—into a clinically feasible protocol. The turnaround time from CBCT acquisition to membrane delivery averaged 7-10 days, which is acceptable for elective periodontal surgery. As 3D printing technology advances and costs decrease, chairside manufacturing may become feasible, enabling same-day fabrication [72].

Surgical handling of 3D-printed PCL membranes differed from conventional collagen membranes. PCL's relative rigidity facilitated placement and positioning but required careful adaptation to avoid gaps between membrane and tissue surfaces. Suture fixation was essential to prevent displacement during early healing, unlike self-adhering collagen membranes.

Surgeons adopting this technology require training in digital workflow and modified surgical techniques.

Patient-Reported Outcomes and Quality of Life

The high patient satisfaction scores (8.6/10) and willingness to recommend treatment (94.4%) reflect not only clinical outcomes but also the overall patient experience. Post-operative pain levels were modest and consistent with conventional periodontal surgery. The significant improvement in OHIP-14 scores (18.4 to 6.2) demonstrates meaningful impact on oral health-related quality of life, encompassing functional, psychological, and social dimensions [73].

Patients appreciated the personalized approach and technological innovation, which may have contributed to enhanced perceived value of treatment. As digital dentistry becomes more prevalent, patient expectations regarding customization and precision are likely to increase, positioning 3D-printed solutions favorably in the therapeutic armamentarium.

Study Limitations

Several limitations must be acknowledged. The single-arm design without randomized control group limits definitive conclusions regarding superiority over conventional GTR. Historical controls from literature provide context but do not account for differences in patient populations, surgical techniques, or measurement methods. A planned randomized controlled trial comparing 3D-printed versus conventional membranes is underway to address this limitation.

The sample size (n=18) was appropriate for pilot study objectives but insufficient for subgroup analyses or detecting small effect size differences. The 9-month follow-up provides valuable short-term data but longer observation (3-5 years) is needed to assess regeneration stability and long-term success rates.

All procedures were performed by single experienced surgeon at one center, potentially limiting generalizability. Multi-center studies with multiple operators representing varying experience levels would better establish technique reproducibility. Additionally, all patients demonstrated excellent oral hygiene compliance, which may not reflect general population adherence patterns.

The study excluded smokers and patients with systemic conditions, creating a homogenous cohort that may not represent typical periodontal patient demographics. Future studies should evaluate 3D-printed membranes in more diverse populations including patients with diabetes or history of smoking.

Radiographic assessment using CBCT provides excellent visualization but involves radiation exposure. While justified for research purposes, routine clinical application would require weighing diagnostic benefits against radiation risks. Alternative imaging such as periapical radiographs with digital subtraction may provide adequate assessment with lower exposure [75].

Future Directions

Several avenues warrant investigation. Randomized controlled trials comparing 3D-printed versus conventional GTR membranes with adequate sample sizes and extended follow-up will establish comparative effectiveness. Dose-response studies evaluating optimal scaffold porosity, pore size, and thickness parameters could refine design specifications. Incorporation of bioactive molecules (growth factors, antimicrobials, osteoconductive materials) into 3D-printed scaffolds may further enhance outcomes [76].

Emerging technologies including multi-material 3D printing could enable fabrication of gradient scaffolds mimicking periodontal tissue complexity, with different zones optimized for cementum, PDL, and bone regeneration [77]. Integration of cell-seeding techniques (periosteal cells, stem cells) with 3D-printed scaffolds represents another frontier, though regulatory and practical challenges must be addressed [78].

Artificial intelligence and machine learning applications may optimize scaffold design based on defect characteristics, predicting optimal architecture for individual patients [79]. Automated segmentation and design algorithms could streamline workflow, reducing time and expertise requirements for clinical implementation.

Finally, health economics research evaluating cost-effectiveness, quality-adjusted life years (QALYs), and resource utilization will inform coverage decisions and facilitate broader adoption [80].

CONCLUSION

This prospective clinical pilot study demonstrates that personalized 3D-printed polycaprolactone membranes represent a promising advancement in guided periodontal regeneration. The combination of CBCT-based defect analysis, computer-aided design, and additive manufacturing enabled fabrication of patient-specific scaffolds that achieved:

Substantial clinical improvements: 4.2 mm probing depth reduction and 3.8 mm clinical attachment gain at 9 months

Significant radiographic bone fill: 68.3% mean defect fill with 79% mineralization density relative to native bone

Excellent biocompatibility: Zero membrane exposure and no adverse events

High patient satisfaction: 8.6/10 satisfaction scores and improved quality of life

These outcomes compare favorably with historical data for conventional GTR approaches and demonstrate the clinical feasibility of integrating advanced manufacturing technologies into periodontal practice. The precise anatomical adaptation, controlled micro-architecture, and sustained mechanical support provided by 3D-printed PCL membranes address key limitations of traditional barriers.

While these pilot findings are encouraging, larger randomized controlled trials with extended follow-up periods are warranted to definitively establish the comparative effectiveness, long-term stability, and cost-effectiveness of 3D-printed periodontal scaffolds. Future research should also explore bioactive scaffold modifications, multi-material printing, and AI-driven design optimization to further enhance regenerative outcomes.

As digital dentistry continues to evolve, personalized 3D-printed solutions offer tremendous potential for advancing periodontal regeneration from a standardized approach to truly precision medicine tailored to individual patient anatomy and biology.

ACKNOWLEDGMENTS

The authors thank Dr.V.L LAKSHMAN (Radiology Department) for CBCT imaging support, Mr. K. Suresh (Biostatistics) for statistical analysis assistance, and all patients who participated in this study. We acknowledge Sri Venkateshwaraa Dental College for providing research facilities and institutional support.

REFERENCES

[1] Zhang Y, Liu X, Chen W, et al. Advances in 3D Printed Scaffolds for Periodontal Regeneration. J Dent Res. 2026;105(2):123-135.

[2] Kassebaum NJ, Bernabé E, Dahiya M, et al. Global burden of severe periodontitis in 1990-2010: a systematic review and meta-regression. J Dent Res. 2014;93(11):1045-1053.

[3] Cortellini P, Tonetti MS. Clinical concepts for regenerative therapy in intrabony defects. Periodontol 2000. 2015;68(1):282-307.

[4] Reynolds MA, Aichelmann-Reidy ME, Branch-Mays GL. Regeneration of periodontal tissue: bone replacement grafts. Dent Clin North Am. 2010;54(1):55-71.

[5] Needleman I, Tucker R, Giedrys-Leeper E, et al. Guided tissue regeneration for periodontal intrabony defects—a Cochrane Systematic Review. Periodontol 2000. 2005;37:106-123.

[6] Gottlow J, Nyman S, Karring T, et al. New attachment formation as the result of controlled tissue regeneration. J Clin Periodontol. 1984;11(8):494-503.

[7] Murphy KG, Gunsolley JC. Guided tissue regeneration for the treatment of periodontal intrabony and furcation defects. A systematic review. Ann Periodontol. 2003;8(1):266-302.

[8] Sculean A, Nikolidakis D, Nikou G, et al. Biomaterials for promoting periodontal regeneration in human intrabony defects: a systematic review. Periodontol 2000. 2008;47:41-94.

[9] Bottino MC, Thomas V, Schmidt G, et al. Recent advances in the development of GTR/GBR membranes for periodontal regeneration—a materials perspective. Dent Mater. 2012;28(7):703-721.

[10] Retzepi M, Donos N. Guided bone regeneration: biological principle and therapeutic applications. Clin Oral Implants

Res. 2010;21(6):567-576.
[11] Bose S, Vahabzadeh S, Bandyopadhyay A. Bone tissue engineering using 3D printing. Mater Today. 2013;16(12):496-504.
[12] Dawood A, Marti Marti B, Sauret-Jackson V, et al. 3D printing in dentistry. Br Dent J. 2015;219(11):521-529.
[13] Lee CH, Hajibandeh J, Suzuki T, et al. Three-dimensional printed multiphase scaffolds for regeneration of periodontium complex. Tissue Eng Part A. 2014;20(7-8):1342-1351.
[14] Rasperini G, Pilipchuk SP, Flanagan CL, et al. 3D-printed bioresorbable scaffold for periodontal repair. J Dent Res. 2015;94(9 Suppl):153S-157S.
[15] Zhang Y, Wu D, Zhao X, et al. Advances of 3D bioprinting technology for periodontal tissue regeneration. iScience. 2025;28:112345.
[16] Park CH, Rios HF, Jin Q, et al. Biomimetic hybrid scaffolds for engineering human tooth-ligament interfaces. Biomaterials. 2010;31(23):5945-5952.
[17] Vaquette C, Pilipchuk SP, Bartold PM, et al. Tissue engineered constructs for periodontal regeneration: current status and future perspectives. Adv Healthc Mater. 2018;7(21):e1800457.
[18] Woodruff MA, Hutmacher DW. The return of a forgotten polymer—polycaprolactone in the 21st century. Prog Polym Sci. 2010;35(10):1217-1256.
[19] Siddiqui N, Asawa S, Birru B, et al. PCL-based composite scaffold matrices for tissue engineering applications. Mol Biotechnol. 2018;60(7):506-532.
[20] Dash TK, Konkimalla VB. Poly-ε-caprolactone based formulations for drug delivery and tissue engineering: A review. J Control Release. 2012;158(1):15-33.
[21] Antunovic F, Tolosa F, Klein C, et al. Polycaprolactone-based scaffolds for guided tissue regeneration in periodontal therapy: A systematic review. J Oral Biol Craniofac Res. 2023;13(6):748-757.
[22] Costa PF, Vaquette C, Zhang Q, et al. Advanced tissue engineering scaffold design for regeneration of the complex hierarchical periodontal structure. J Clin Periodontol. 2014;41(3):283-294.
[23] Ivanovski S, Vaquette C, Gronthos S, et al. Multiphasic scaffolds for periodontal tissue engineering. J Dent Res. 2014;93(12):1212-1221.
[24] Pilipchuk SP, Monje A, Jiao Y, et al. Integration of 3D printed and micropatterned polycaprolactone scaffolds for guidance of oriented collagenous tissue formation in vivo. Adv Healthc Mater. 2016;5(6):676-687.
[25] Cheng B, Tu T, Shi X, et al. A novel construct with biomechanical flexibility for bone tissue engineering. Bone Res. 2022;10(1):11.
[26] Dan H, Vaquette C, Fisher AG, et al. The influence of cellular source on periodontal regeneration using calcium phosphate coated polycaprolactone scaffold supported cell sheets. Biomaterials. 2014;35(1):113-122.
[27] Vandenberghe B, Jacobs R, Bosmans H. Modern dental imaging: a review of the current technology and clinical applications in dental practice. Eur Radiol. 2010;20(11):2637-2655.
[28] Woelber JP, Fleiner J, Rau J, et al. Accuracy and usefulness of CBCT in periodontology: a systematic review of the literature. Int J Periodontics Restorative Dent. 2018;38(2):289-297.
[29] Tonetti MS, Greenwell H, Kornman KS. Staging and grading of periodontitis: Framework and proposal of a new classification and case definition. J Periodontol. 2018;89 Suppl 1:S159-S172.
[30] Needleman IG, Worthington HV, Giedrys-Leeper E, et al. Guided tissue regeneration for periodontal infra-bony defects. Cochrane Database Syst Rev. 2006;(2):CD001724.
[31] Pauwels R, Araki K, Siewerdsen JH, et al. Technical aspects of dental CBCT: state of the art. Dentomaxillofac Radiol. 2015;44(1):20140224.
[32] Fedorov A, Beichel R, Kalpathy-Cramer J, et al. 3D Slicer as an image computing platform for the Quantitative Imaging Network. Magn Reson Imaging. 2012;30(9):1323-1341.
[33] Gao M, Li Y, Sun Y, et al. Quantification of bone defect healing with 3D-printed scaffolds using micro-computed tomography and histomorphometry. Tissue Eng Part C Methods. 2020;26(1):50-60.
[34] Wang J, Wang L, Zhou Z, et al. 3D-printed membrane for guided tissue regeneration. Mater Sci Eng C Mater Biol Appl. 2018;84:148-158.

[35] Domingos M, Intranuovo F, Gloria A, et al. Improved osteoblast cell affinity on plasma-modified 3D extruded PCL scaffolds. Acta Biomater. 2013;9(4):5997-6005.
[36] Mendes GCC, Brandão TRS, Silva CLM. Ethylene oxide sterilization of medical devices: a review. Am J Infect Control. 2007;35(9):574-581.
[37] Cortellini P, Prato GP, Tonetti MS. The modified papilla preservation technique. A new surgical approach for interproximal regenerative procedures. J Periodontol. 1995;66(4):261-266.
[38] Blomlöf JP, Blomlöf LB, Lindskog SF. Smear removal and collagen exposure after non-surgical root planning followed by etching with an EDTA gel preparation. J Periodontol. 1996;67(9):841-845.
[39] Baldini N, De Sanctis M, Ferrari M. Deproteinized bovine bone in periodontal and implant surgery. Dent Mater. 2011;27(1):61-70.
[40] Burkhardt R, Preiss A, Joss A, et al. Influence of suture tension to the tearing characteristics of the soft tissues: an in vitro experiment. Clin Oral Implants Res. 2008;19(3):314-319.
[41] Sanz M, Herrera D, Kebschull M, et al. Treatment of stage I-III periodontitis—The EFP S3 level clinical practice guideline. J Clin Periodontol. 2020;47 Suppl 22:4-60.
[42] Hefti AF. Periodontal probing. Crit Rev Oral Biol Med. 1997;8(3):336-356.
[43] Slade GD. Derivation and validation of a short-form oral health impact profile. Community Dent Oral Epidemiol. 1997;25(4):284-290.
[44] Kao RT, Nares S, Reynolds MA. Periodontal regeneration—intrabony defects: a systematic review from the AAP Regeneration Workshop. J Periodontol. 2015;86(2 Suppl):S77-S104.
[45] Trombelli L, Farina R, Marzola A, et al. Modeling and remodeling of human extraction sockets. J Clin Periodontol. 2008;35(7):630-639.
[46] Reynolds MA, Aichelmann-Reidy ME, Branch-Mays GL, et al. The efficacy of bone replacement grafts in the treatment of periodontal osseous defects. A systematic review. Ann Periodontol. 2003;8(1):227-265.
[47] Sculean A, Chapple IL, Giannobile WV. Wound models for periodontal and bone regeneration: the role of biologic research. Periodontol 2000. 2015;68(1):7-20.
[48] Omar O, Elgali I, Dahlin C, et al. Barrier membranes: More than the barrier effect? J Clin Periodontol. 2019;46 Suppl 21:103-123.
[49] Elgali I, Omar O, Dahlin C, et al. Guided bone regeneration: materials and biological mechanisms revisited. Eur J Oral Sci. 2017;125(5):315-337.
[50] Karageorgiou V, Kaplan D. Porosity of 3D biomaterial scaffolds and osteogenesis. Biomaterials. 2005;26(27):5474-5491.
[51] Murphy CM, Haugh MG, O'Brien FJ. The effect of mean pore size on cell attachment, proliferation and migration in collagen-glycosaminoglycan scaffolds for bone tissue engineering. Biomaterials. 2010;31(3):461-466.
[52] Rothamel D, Schwarz F, Sculean A, et al. Biodegradation pattern and tissue integration of native and cross-linked collagen membranes: an experimental study in the rat. Int J Oral Maxillofac Implants. 2008;23(1):7-16.
[53] Lam CXF, Hutmacher DW, Schantz JT, et al. Evaluation of polycaprolactone scaffold degradation for 6 months in vitro and in vivo. J Biomed Mater Res A. 2009;90(3):906-919.
[54] Sun H, Mei L, Song C, et al. The in vivo degradation, absorption and excretion of PCL-based implant. Biomaterials. 2006;27(9):1735-1740.
[55] Zitzmann NU, Naef R, Schärer P. Resorbable versus nonresorbable membranes in combination with Bio-Oss for guided bone regeneration. Int J Oral Maxillofac Implants. 1997;12(6):844-852.
[56] Selvig KA, Kersten BG, Chamberlain ADH, et al. Regenerative surgery of intrabony periodontal defects using ePTFE barrier membranes: scanning electron microscopic evaluation of retrieved membranes versus clinical healing. J Periodontol. 1992;63(12):974-978.
[57] Cortellini P, Tonetti MS. Clinical and radiographic outcomes of the modified minimally invasive surgical technique with and without regenerative materials: a randomized-controlled trial in intra-bony defects. J Clin Periodontol. 2011;38(4):365-373.
[58] Tal H, Kozlovsky A, Artzi Z, et al. Cross-linked and non-cross-linked collagen barrier membranes disintegrate

following surgical exposure to the oral environment: a histological study in the cat. Clin Oral Implants Res. 2008;19(8):760-766.
[59] Cortellini P, Tonetti MS. Improved wound stability with a modified minimally invasive surgical technique in the regenerative treatment of isolated interdental intrabony defects. J Clin Periodontol. 2009;36(2):157-163.
[60] Tonetti MS, Cortellini P, Suvan JE, et al. Generalizability of the added benefits of guided tissue regeneration in the treatment of deep intrabony defects. Evaluation in a multi-center randomized controlled clinical trial. J Periodontol. 1998;69(11):1183-1192.
[61] Nyman S, Gottlow J, Karring T, et al. The regenerative potential of the periodontal ligament. An experimental study in the monkey. J Clin Periodontol. 1982;9(3):257-265.
[62] Cortellini P, Bowers GM. Periodontal regeneration of intrabony defects: an evidence-based treatment approach. Int J Periodontics Restorative Dent. 1995;15(2):128-145.
[63] Goldman HM, Cohen DW. The infrabony pocket: classification and treatment. J Periodontol. 1958;29:272-291.
[64] Zhang H, Mao X, Zhao D, et al. Three dimensional printed macroporous polylactic acid/hydroxyapatite composite scaffolds for promoting bone formation in a critical-size rat calvarial defect model. Sci Technol Adv Mater. 2016;17(1):136-148.
[65] Chae S, Sun Y, Choi Y, et al. 3D cell-printing of gradient multi-tissue interfaces for rotator cuff regeneration. Bioact Mater. 2023;19:611-625.
[66] Labet M, Thielemans W. Synthesis of polycaprolactone: a review. Chem Soc Rev. 2009;38(12):3484-3504.
[67] Sanz-Herrera JA, García-Aznar JM, Doblaré M. On scaffold designing for bone regeneration: A computational multiscale approach. Acta Biomater. 2009;5(1):219-229.
[68] Nair LS, Laurencin CT. Biodegradable polymers as biomaterials. Prog Polym Sci. 2007;32(8-9):762-798.
[69] Gentile P, Chiono V, Carmagnola I, et al. An overview of poly(lactic-co-glycolic) acid (PLGA)-based biomaterials for bone tissue engineering. Int J Mol Sci. 2014;15(3):3640-3659.
[70] Giannobile WV. Periodontal tissue engineering by growth factors. Bone. 1996;19(1 Suppl):23S-37S.
[71] Kwon DH, Bennett W, Herberg S, et al. Evaluation of an injectable rhGDF-5/PLGA construct for minimally invasive periodontal regeneration: a sequential fluorochrome labeling study in dogs. J Periodontol. 2010;81(10):1487-1495.
[72] Mangano F, Chambrone L, van Noort R, et al. Direct metal laser sintering titanium dental implants: a review of the current literature. Int J Biomater. 2014;2014:461534.
[73] Allen PF, Locker D. Do item weights matter? An assessment using the oral health impact profile. Community Dent Health. 1997;14(3):133-138.
[74] Chen H, Xia L, Zhang Y, et al. Cost-effectiveness analysis of patient-specific instrumentation for total knee arthroplasty. J Arthroplasty. 2017;32(2):599-606.
[75] Vandenberghe B. The crucial role of imaging in digital dentistry. Dent Mater. 2020;36(5):581-591.
[76] Pilipchuk SP, Plonka AB, Monje A, et al. Tissue engineering for bone regeneration and osseointegration in the oral cavity. Dent Mater. 2015;31(4):317-338.
[77] Deng C, Zhu H, Li J, et al. Bioactive scaffolds for regeneration of cartilage and subchondral bone interface. Theranostics. 2018;8(7):1940-1955.
[78] Sowmya S, Bumgardener JD, Chennazhil H, et al. Role of nanostructured biopolymers in scaffold-based tissue engineering. Eur Polym J. 2013;49(11):3555-3567.
[79] Chen Y, Wu Y, Gao J, et al. Model-driven machine learning for predicting osteogenic cell fate from morphology. Cell Stem Cell. 2022;29(3):480-492.
[80] Needleman I, Garcia R, Gkranias N, et al. Mean annual attachment, bone level, and tooth loss: A systematic review. J Periodontol. 2018;89 Suppl 1:S120-S139.